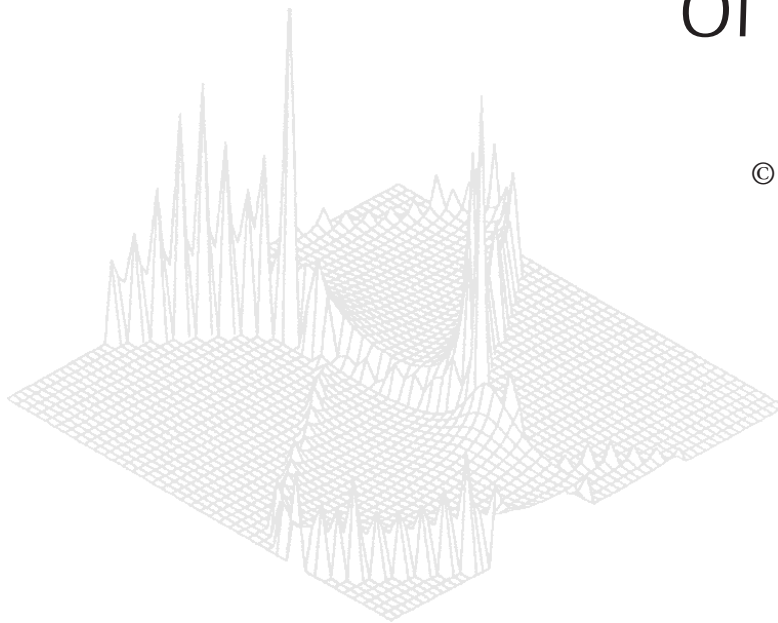

C S I R O P U B L I S H I N G

Australian Journal of Physics

Volume 50, 1997
© CSIRO Australia 1997



A journal for the publication of
original research in all branches of physics

www.publish.csiro.au/journals/ajp

All enquiries and manuscripts should be directed to

Australian Journal of Physics

CSIRO PUBLISHING

PO Box 1139 (150 Oxford St)

Collingwood

Vic. 3066

Australia

Telephone: 61 3 9662 7626

Facsimile: 61 3 9662 7611

Email: peter.robertson@publish.csiro.au



Published by **CSIRO PUBLISHING**
for CSIRO Australia and
the Australian Academy of Science



Space Weather, SuperDARN and the Tasmanian Tiger*

Raymond A. Greenwald

Applied Physics Laboratory, The Johns Hopkins University,
Johns Hopkins Road, Laurel, MD 20723, USA.

Abstract

The plasma environment extending from the solar surface through interplanetary space to the outermost reaches of the Earth's atmosphere and magnetic field is dynamic, often disturbed, and capable of harming humans and damaging manmade systems. Disturbances in this environment have been identified as space weather disturbances. At the present time there is growing interest in monitoring and predicting space weather disturbances. In this paper we present some of the difficulties involved in achieving this goal by comparing the processes that drive tropospheric-weather systems with those that drive space-weather systems in the upper atmosphere and ionosphere. The former are driven by pressure gradients which result from processes that heat and cool the atmosphere. The latter are driven by electric fields that result from interactions between the streams of ionised gases emerging from the Sun (solar wind) and the Earth's magnetosphere. Although the dimensions of the Earth's magnetosphere are vastly greater than those of tropospheric weather systems, the global space-weather response to changes in the solar wind is much more rapid than the response of tropospheric-weather systems to changing conditions. We shall demonstrate the rapid evolution of space-weather systems in the upper atmosphere through measurements with a global network of radars known as SuperDARN. We shall also describe how the SuperDARN network is evolving, including a newly funded Australian component known as the Tasman International Geospace Environmental Radar (TIGER).

1. Introduction

Just as the Sun has a fundamental influence on the Earth's climate and weather, it also has a fundamental influence on the plasma (ionised gas) environment in interplanetary space and in the Earth's immediate neighbourhood. In fact, the Earth is embedded in the outermost reaches of the solar atmosphere and subjected to a continual stream of low energy (few electron volts) plasma flowing outward from the Sun at a velocity of hundreds of kilometres per second as well as sporadic intensifications of very energetic particles associated with particularly strong solar eruptions. This dynamic plasma environment is commonly called the solar wind. The Earth is protected from the solar wind by its magnetic field which forms a cavity that extends to $\sim 70,000$ in the sunward direction and $\sim 10^6$ km in the antisunward direction. The boundary region is referred to as the magnetopause

* Refereed paper based on a plenary lecture given at the 12th Australian Institute of Physics Congress, held at the University of Tasmania, Hobart, in July 1996.

and the cavity itself is referred to as the magnetosphere. The magnetosphere is divided into distinct plasma environments. At high altitudes, the magnetospheric plasma is very tenuous and has a characteristic energy ranging to tens of kilovolts. At lower latitudes, the plasma densities increase and the characteristic energies decrease, until at the lower boundary of the magnetosphere, the ionosphere, the characteristic energy of the plasma is only a few tenths of an electron volt and it is only partially ionised. There, at altitudes of 100–1000 km, it merges with the uppermost reaches of the Earth's atmosphere.

While the magnetopause shields the Earth's magnetosphere from most of the solar wind flux incident upon it, it does allow a transfer of some of the solar wind energy, momentum and mass flux. The processes associated with this transfer are not yet fully understood, but they do generate large-scale current systems that distort the shape of the magnetosphere, and they generate large-scale electric and magnetic fields that energise the magnetospheric plasma populations and cause large-scale circulation of the magnetospheric plasma. Many of the currents are footed in the ionosphere at high latitudes where they dissipate their energy in the upper atmosphere in the form of particle and Joule heating. Also, the circulation patterns that are excited in the magnetosphere are imaged in the ionosphere at high latitudes. Thus, disturbances on the Sun lead to disturbances in interplanetary space, the magnetosphere and the ionosphere. The variable state of the plasma in these different regimes may be considered as analogous to changing meteorological conditions in the Earth's lower atmosphere. We typically speak of varying meteorological conditions as weather. The analogy for the varying plasma environments of interplanetary space, the magnetosphere, and the ionosphere is space weather.

Disturbed meteorological conditions can have a devastating impact on humans and human activities. Similar devastation can arise from space-weather disturbances. In the most extreme case, the radiation associated with a major solar flare could kill an astronaut in interplanetary space. At a lesser though still important level of significance, major flares do damage satellite electronics even when the satellites are located within the Earth's magnetosphere. Major solar storms lead to increased energy dissipation in the upper atmosphere, thereby increasing the scale height of the atmosphere and atmospheric drag on satellites in low Earth orbit. The results are decreased satellite lifetime and temporary loss of satellite location. Major storms also lead to very strong current surges in the ionosphere at high latitudes which induce current surges in power grids that lead to the destruction of power transformers. Finally, all storms cause disturbances in the ionosphere and thereby affect HF and satellite communications. These ionospheric effects are particularly noticeable at high latitudes where the precipitating energetic particles associated with auroras produce considerable ionospheric structure and can cause absorption of radiowave signals.

The impact of disturbed space weather conditions on human technological systems is particularly noticeable at high latitudes. This arises because the magnetospheric domains most strongly affected by disturbances in the solar wind are magnetically connected by geomagnetic field lines to the high-latitude ionosphere. Thus, energised magnetospheric plasma precipitates along magnetic field lines into the high-latitude ionosphere, magnetospheric currents flow along magnetic field lines into the ionosphere, and magnetospheric electric fields map

along equipotential magnetic field lines into the ionosphere producing a compact view of the circulation patterns of the magnetospheric plasma. The high-latitude ionosphere then becomes a viewing screen on which one can observe on a global scale the spatial and temporal evolution of space-weather disturbances within the magnetosphere.

To date, the global-scale auroral precipitation patterns have been observed with satellite-borne imagers operating at ultraviolet and visible wavelengths (e.g. Frank and Craven 1988; Murphree *et al.* 1991), while field-aligned current flow and electric fields have only been observed statistically for characteristic directions of the magnetic field in the solar wind (e.g. Potemra 1994; Heppner and Maynard 1987). Recently, however, a new network of high-latitude radars has been developed to study the spatial and temporal evolution of magnetospheric plasma circulation on a global scale. These circulation patterns are the space-weather analog of atmospheric circulation associated with meteorological weather systems. It is interesting to compare the measurement requirements and the techniques that are used to study the atmospheric circulation associated with continental-scale weather systems and the magnetospheric/ionospheric circulation associated with space-weather disturbances. This is the primary subject of this paper. In developing this topic, we will also describe the Super Dual Auroral Radar Network (SuperDARN) and its recent contributions to global-scale measurements of plasma winds in the high-latitude ionosphere.

2. Comparison of Winds in the Lower Atmosphere and Plasma Winds

(2a) Scale Size of the Phenomena

Both atmospheric and plasma wind systems may be divided into four distinct categories based on scale size. Planetary-scale winds in the lower atmosphere are wind systems that are determined by the largest features of global circulation. They are driven by solar heating of the atmosphere and modified by continental boundaries and orographic features. Synoptic-scale winds are the wind systems associated with day-to-day weather systems. They have dimensions of hundreds to thousands of kilometres and are associated with more localised sources of atmospheric heating and cooling that cause weather related high and low pressure systems. Mesoscale winds are associated with even more localised sources of atmospheric heating and cooling. They have horizontal dimensions of tens to hundreds of kilometres and are related to smaller jet streams, squall lines and lee waves. Finally, small-scale winds have dimensions of kilometres or less. This category includes small-scale wind structure, convective clouds and tornadoes. Planetary-scale, synoptic-scale and mesoscale winds are essentially horizontal in character. Small-scale wind structures can have considerable vertical wind structure as is the case in tornadoes.

Planetary-scale plasma winds are driven by global atmospheric circulation at high altitudes. The circulation is driven by solar heating and, because of the altitude, is not affected by continental boundaries or orographic features. Synoptic-scale plasma winds are the wind systems associated with space-weather effects and they occur because of coupling of momentum from the solar wind to the magnetosphere. These systems have dimensions of thousands of kilometres. One example is the two-cell convection pattern that occurs at high latitudes when

there is good electromagnetic coupling between the solar wind and the Earth's magnetosphere. This pattern is characterised by antisunward winds across the polar cap and sunward winds at lower latitudes. Momentum is transferred from this plasma wind pattern to the neutral atmosphere producing a similar circulation pattern in the upper atmosphere. Mesoscale plasma winds have dimensions of hundreds of kilometres. They are associated with magnetohydrodynamic waves, structured auroral surges and vortices. In general, these features are images of magnetospheric processes. Small-scale plasma winds have dimensions of tens of kilometres or less. They may be driven by processes occurring in the magnetosphere or the ionosphere and they include phenomena such as winds associated with individual auroral arcs and plasma instabilities. Plasma winds at all scale sizes are directed orthogonal to the geomagnetic field. At high latitudes the circulation is approximately horizontal.

(2b) Defining Equations

The horizontal equation of motion for winds in the lower atmosphere with the neglect of centrifugal and frictional effects is given by

$$d\mathbf{u}/dt = -\nabla p/\rho - 2\boldsymbol{\Omega} \times \mathbf{u}, \quad (1)$$

where Ω is the angular rotation frequency of the Earth, $d\mathbf{u}/dt = \partial\mathbf{u}/\partial t + \mathbf{u} \cdot \nabla\mathbf{u}$ is the convective derivative, p is the pressure, \mathbf{u} the horizontal velocity and ρ the mass density. It can be seen that two terms affect the acceleration of a parcel of air: pressure gradients and the Coriolis acceleration. In general, the inertial effects on the left-hand side of the equation may be ignored on time scales of the order of one day.

The acceleration due to pressure gradients is small. For example, 1 mB of pressure variation over 100 km yields an acceleration of $8 \times 10^{-4} \text{ m s}^{-2}$. Using the previous approximations, the acceleration due to the pressure gradient is balanced by the Coriolis acceleration and the horizontal wind is given by

$$\mathbf{u} = \boldsymbol{\Omega} \times \nabla p / 2\Omega^2 \rho. \quad (2)$$

This wind is commonly referred to as the geostrophic wind. It is the wind flowing on the surface of a rotating body, where the wind is driven by pressure gradients, but ultimately is controlled by the Coriolis force. In a steady state, the wind flows at right angles to the forcing term which is the pressure gradient. The flow pattern represents the counterclockwise (clockwise) wind circulation about high (low) pressure systems in the southern hemisphere. In the northern hemisphere the sense of circulation is reversed. For the case of winds in the lower atmosphere, the time constant to reach this steady state is approximately one day. We should note, moreover, that the pressure distributions generally change slowly as they move across continental land masses and, therefore, the actual wind pattern is generally close to that given by (2).

Equation (2) may also be written in a slightly more formal fashion as

$$\mathbf{u} = \boldsymbol{\Omega} \times \nabla \Phi / 2\Omega^2, \quad (3)$$

where $\Phi = p/\rho$ is the geopotential.

Plasma winds in the upper atmosphere are controlled by electromagnetic forces. Since plasmas always contain at least two species with positive or negative charge, the equation of motion for the j th species for the component of motion orthogonal to the magnetic field is given by

$$d\boldsymbol{\nu}_j/dt = -\nabla p_j/\rho_j + (q_j/m_j)(\mathbf{E} + \boldsymbol{\nu}_j \times \mathbf{B}) + \nu_{jn}(\boldsymbol{\nu}_j - \mathbf{u}), \quad (4)$$

where ν_{jn} is the collision frequency with neutrals of the j th species, and q_j and m_j are the charge and mass of the j th species. The first term on the right-hand side of the equation is the acceleration due to pressure gradients, the second term is the acceleration due to electromagnetic forces, and the third the acceleration due to frictional forces. In the upper atmosphere above 150 km altitude, frictional forces are negligible for all charge species. Also, comparison of the magnitudes of anticipated pressure gradient and electromagnetic forces shows that the latter are much more significant. For example, assuming a nominal auroral zone electric field of 20 mV m^{-1} yields an acceleration due to the electric field of $1.2 \times 10^5 \text{ m s}^{-1}$. This acceleration is eight orders of magnitude larger than the acceleration due to pressure gradients in the lower atmosphere.

Again ignoring the inertial terms on the left-hand side of (4), we find that the only significant term in the equation is the electromagnetic term. This may be solved to yield

$$\boldsymbol{\nu}_j = (q_j/m_j)\boldsymbol{\omega}_j \times \nabla\phi/\omega_j^2, \quad (5)$$

where $\boldsymbol{\omega}_j = q_j \mathbf{B}/m_j$ is the cyclotron frequency of species j , and ϕ is the electrical potential. It can be seen that (3) and (5) are formally identical. In the former, the acceleration is via geopotential gradients; in the latter, it is via electrical potential gradients. In both cases the direction of the wind is orthogonal to the direction of the potential gradient. We have already seen that the magnitude of the acceleration is far greater in the case of electromagnetic forces. Also, the response time is much less. The cyclotron period which is to be compared with the rotation period of the Earth ranges from 30 ms for molecular ions to 100 ns for electrons. What we have not shown is that the high-latitude electrical potential distribution in the ionosphere can change dramatically on a global scale on time scales of minutes in response to changing solar wind conditions. Thus, the high-latitude plasma wind patterns are very dynamic and a clear indicator of our space-weather environment.

(2c) Monitoring Lower Atmospheric and Plasma Winds

Weather conditions in the lower atmosphere are typically monitored with radiosonde balloons that are launched at regular intervals on a worldwide basis. The balloons measure pressure, temperature and humidity. From their location and motion, it is also possible to obtain altitude and wind velocity. Using these data, meteorologists can determine continental-scale maps of atmospheric conditions at specific altitudes or pressure levels and from these track and forecast weather conditions across a continent. For example, Fig. 1 shows an example of winds and temperatures over North America at a pressure level of 500 mb on 20 November 1964. The solid contours represent the geopotential

altitude of the 500 mb level at spacings of 60 m. The geopotential altitudes are indicated in tens of metres and range from ~ 5000 – 5800 m. The dashed contours represent the temperatures in degrees Celsius at the same pressure level. The lowest temperatures occur at the lowest geopotential altitudes indicating that these are regions of cold dense air that have collapsed toward the surface. They represent the low pressure regions on a weather map. The contours with the highest temperatures and highest geopotential altitudes correspond to high pressure regions. Finally, the map shows wind velocity in knots at the 500 mb level. The velocity is indicated by the small flag. Each black triangle is 50 knots, each full vertical line is 10 knots and each short vertical line is 5 knots. The extending horizontal line indicates the direction of flow. It can readily be seen that the winds flow along constant geopotential contours and that they have a counterclockwise circulation about the low pressure centre. This is exactly as would be expected in the northern hemisphere.

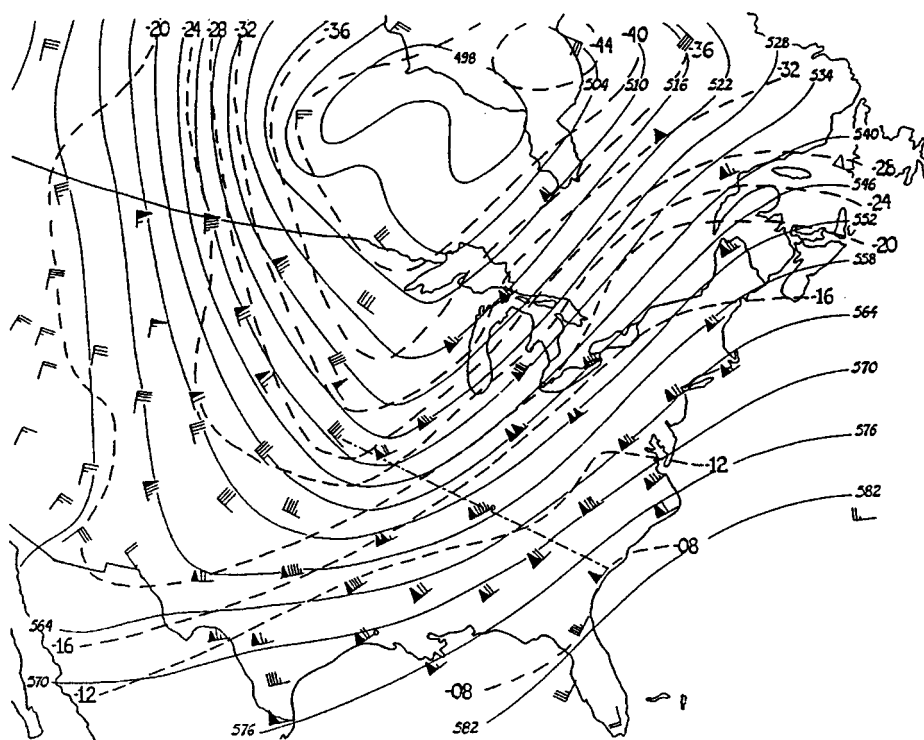


Fig. 1. Atmospheric conditions over North America at a pressure level of 500 mb as obtained from radiosonde observations on 20 November 1964 at 00 UT. The solid contours represent geopotential height contours in tens of metres, the dashed contours represent isotherms in degrees Celsius, and the flags indicate wind direction and magnitude. Note that the wind direction is generally aligned with the geopotential contours (from Wallace and Hobbs 1977).

Fig. 2 shows four geopotential maps over North America obtained at intervals of 12 hours for the interval from 00 UT on 19 November 1964 to 12 UT on 20 November 1964. The low pressure system is fairly stationary over central Canada whereas there is some development of the high pressure system across

the southern United States. It is fairly clear that these geopotential maps change fairly slowly as weather systems migrate across North America. Radiosonde observations need only be made infrequently, but for each set of observations a large number of balloons, indicated by the wind flags in Fig. 1, must be launched and tracked. Although these data were obtained in 1964, radiosonde balloons still remain the primary technique for monitoring conditions in the lower atmosphere on a continental scale.

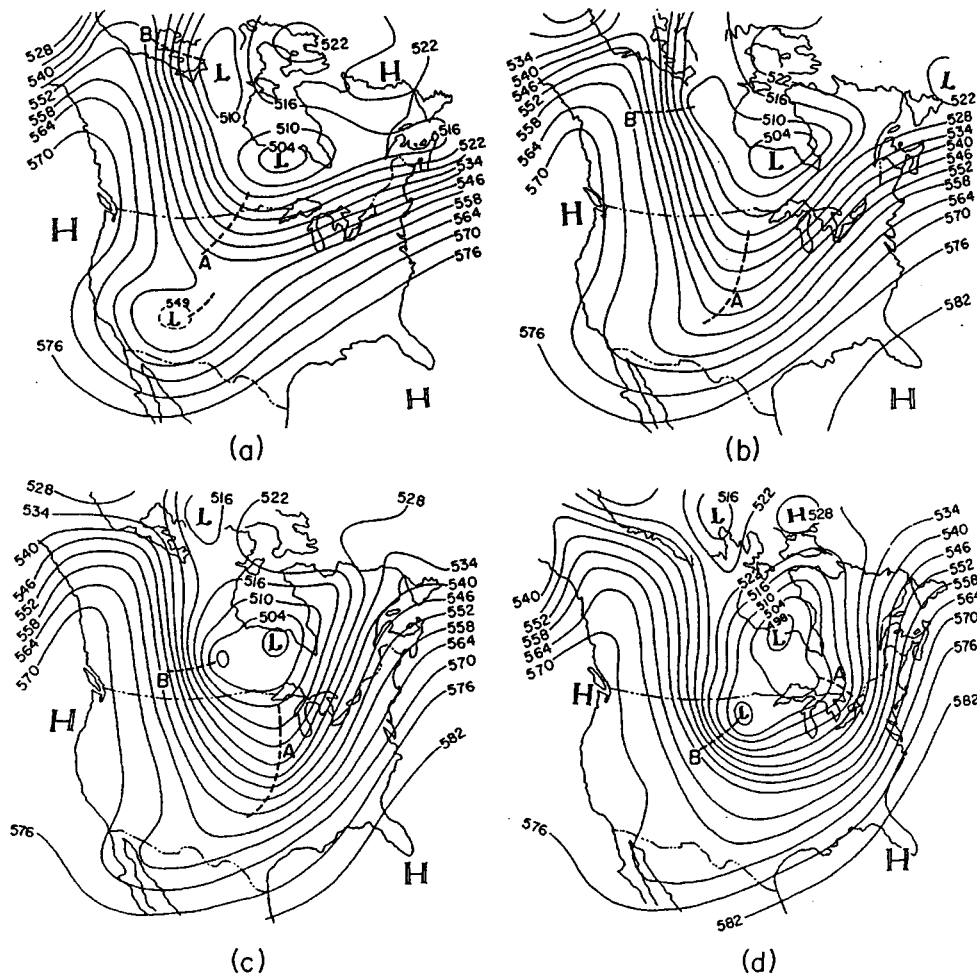


Fig. 2. Four sequential maps of geopotential height at the 500 mb pressure level as observed at 12-hour intervals over North America from 00 UT on 19 November 1964 to 12 UT on 20 November 1964. Height contours are given in tens of metres. Note that the contours maps change relatively slowly (from Wallace and Hobbs 1977).

Plasma winds in the upper atmosphere have been observed directly or in terms of the associated potential electric field via a number of techniques, including electric field antennas on stratospheric balloons (e.g. Mozer and Serlin 1969), sounding rockets (e.g. Fahleson 1967) and satellites (e.g. Mozer 1973); plasma

drift instruments on satellites (e.g. Heelis *et al.* 1981), and ground-based radars (e.g. Banks and Doupnik 1975; Ruohoniemi *et al.* 1987). Until recently, most of these measurements were of limited duration, limited spatial coverage or limited local time coverage. Balloons provide single point observations of the fringing electric field at stratospheric altitudes for intervals ranging from days to weeks, rockets provide measurements along the trajectory for intervals of 10–15 minutes, satellites provide full orbit data, but only at the local times of the orbit plane, and coherent and incoherent scatter radars provide meridional and/or two-dimensional measurements of plasma motions in the ionosphere near the radar site. At times, single radars have provided fairly extensive spatial coverage (e.g. Evans *et al.* 1979; Greenwald *et al.* 1990), allowing a glimpse of the instantaneous global plasma wind pattern. There have also been statistical studies of the global plasma wind pattern using satellite and radar data. Of particular note are the statistical satellite investigations of Heppner and Maynard (1987), Rich and Hairston (1994) and Weimer (1995) and the statistical Goose Bay radar investigation of Ruohoniemi and Greenwald (1996). In general, these investigations have shown a strong dependence of the average plasma wind pattern on the orientation of the interplanetary magnetic field (IMF). While the results have been consistent with theoretical and modeling studies by many authors, the question remains as to how these patterns evolve on a global basis in response to a changing orientation of the IMF.

Recently, a network of HF coherent scatter radars operating under the acronym SuperDARN (Super Dual Auroral Radar Network) has been under development to provide a global view of plasma winds in the high-latitude ionospheres of both hemispheres (Greenwald *et al.* 1995). The goals of the network are severalfold, but most importantly to understand the spatial and temporal evolution of the global high-latitude electrical potential pattern and thereby improve our understanding of solar-wind/magnetosphere/ionosphere coupling processes and the factors and processes that affect space weather. The previous comparison of lower atmospheric and plasma winds has shown that a monitoring network for plasma winds must respond to global changes in the electrical potential distribution across the polar caps on time scales of minutes. The measurements must also be of sufficiently high spatial density that they can resolve the physical processes under investigation and they must have adequate temporal continuity to track the evolution of the system. The SuperDARN radar network responds to all of these requirements and is currently providing unique views of global-scale plasma winds.

(2d) Plasma Wind Observations with SuperDARN

Elements of the SuperDARN radar network have been operational since the summer of 1993. Since that time the data have been used for a broad range of studies relating to the structure and temporal evolution of plasma winds in the high-latitude ionosphere. We present here a few examples of some of this work in order to demonstrate the dynamic nature of these winds and space-weather processes, in general. We will also present some examples of simultaneous, magnetically-conjugate observations of plasma winds in the polar regions of the northern and southern hemisphere as obtained with HF radars that eventually became elements of SuperDARN. These observations display a synchronism of response that reinforces the global dynamic nature of space-weather phenomena.

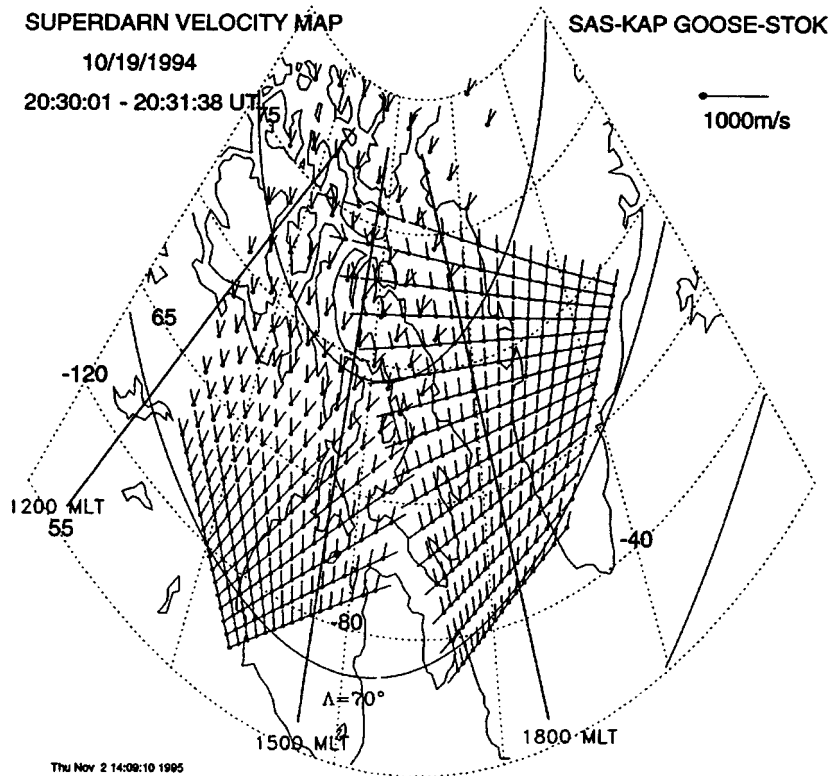


Fig. 3. Map of northeastern Canada and Greenland showing overlapping fields of view of four of the northern-hemisphere SuperDARN radars. The radars provide vector determinations of the cross hatched areas. The more westerly field-of-view is for the radars in Saskatoon, Saskatchewan and Kapuskasing, Ontario, while the more easterly field-of-view is for the radars at Goose Bay, Labrador and Stokkseyri, Iceland (from Greenwald *et al.* 1996).

Fig. 3 shows a map of eastern Canada and Greenland upon which the fields of view of four of the SuperDARN radars (Saskatoon, Kapuskasing, Goose Bay and Stokkseyri) are superposed as cross hatched areas. It can be seen that the radars operate in pairs sharing common viewing areas. The radars are sensitive to small-scale F-region ionospheric irregularities that are extended along magnetic field lines and move transversely to the magnetic field in response to the ionospheric electric field as indicated by (4). The irregularities have a large radar cross section and can therefore be easily sensed with a radar of modest power level. In order to sense the irregularities, the radar wave vector must be orthogonal to the magnetic field within the scattering region. In general, radars operating at frequencies above 30 MHz are unable to meet this requirement at high latitudes due to geometric constraints. However, radars operating in the HF frequency band achieve this condition due to ionospheric refraction. The process is directly related to the use of HF frequencies for shortwave communications, radio broadcasting and over-the horizon radar detection. As the radar signals are scattered they are Doppler shifted due to the motion of the irregularities. Since the irregularity motion is confined to the plane perpendicular to the magnetic

field, observations are only required from two directions in order to determine the velocity vector. Measurements by Ruohoniemi *et al.* (1987) have shown that these irregularity motions may be directly related to plasma winds in the F-region of the high-latitude ionosphere.

It should be noted here that the SuperDARN radars do not detect backscatter from everywhere within their fields of view. This is due to the facts that irregularities are not formed everywhere within a radar's field-of-view and that the orthogonality condition is not achieved everywhere within a radar's field-of-view. Backscatter is only detected from spatial regions in which both conditions are fulfilled concurrently. In general, this occurs sufficiently often that the SuperDARN radars provide valuable and unique contributions to the study of plasma winds at high latitudes.

Fig. 4 shows a sequence of four plasma wind maps obtained with the four radars identified in Fig. 3. The maps were formed every 100 s and show the evolution of the plasma wind pattern in the early afternoon local-time sector over a seven minute interval. The spatial area covered by these maps is approximately equal to the land area of Australia. The gross feature observed is the dusk plasma convection cell. It is indicated by westward plasma winds near 18 MLT and poleward plasma winds from 12–15 MLT. However, superimposed on this large-scale structure is a smaller-scale convection vortex located near 15 MLT and 75° magnetic latitude. This feature is very dynamic, changing appreciably on time scales of 100 s and disappearing entirely in association with the onset of significant auroral precipitation in the midnight local time sector (Greenwald *et al.* 1996). Thus, it can be seen that plasma winds can effectively be viewed over large spatial dimension with ground-based radars and that plasma wind systems are much more dynamic than their neutral gas counterparts in the lower atmosphere.

A second example of the use of radars to detect dynamic variations in plasma wind systems is shown in Fig. 5 (from Greenwald *et al.* 1990). In this example, wind measurements are presented from a pair of radars located at opposite ends of a geomagnetic field line. Each radar only provides a single Doppler component, so the vector patterns shown here are only approximate. They are derived from the azimuthal variation of the Doppler measurements and the knowledge that the plasma-wind pattern is divergence free. Freeman *et al.* (1991) have discussed the types of error that may result from this approach. Keeping in mind that some error may be present in the patterns we can nevertheless compare simultaneous observation of plasma winds near noon in the northern and southern polar regions. It can be seen that the Goose Bay radar observes westward plasma wind near noon in the northern hemisphere, whereas the Halley radar observes eastward plasma wind in the southern hemisphere at the same time with some westward plasma motion at lower latitudes. This complementary flow configuration is due to the dawn–dusk component of the interplanetary magnetic field (IMF) and had been reported on the basis of empirical studies of satellite data sets (Heppner and Maynard 1987) and theoretical models (e.g. Crooker 1979). What had not been observed or reported was the manner in which the flow pattern changes. Fig. 6 shows the variation of the plasma-wind pattern near noon as the dawn–dusk component of the IMF changed from duskward ($B_y > 0$) to dawnward ($B_y < 0$). Each image has an integration time of 100 s. It can be seen that the new

wind pattern begins to form at the equatorward edge of the preexisting pattern and expands poleward filling the radar field of view. Typically, the new wind pattern is completely reconfigured over 10^6 km^2 within 6 minutes of the start of the reconfiguration. The rapidity of this change over a large spatial area is unmatched in the lower atmosphere.

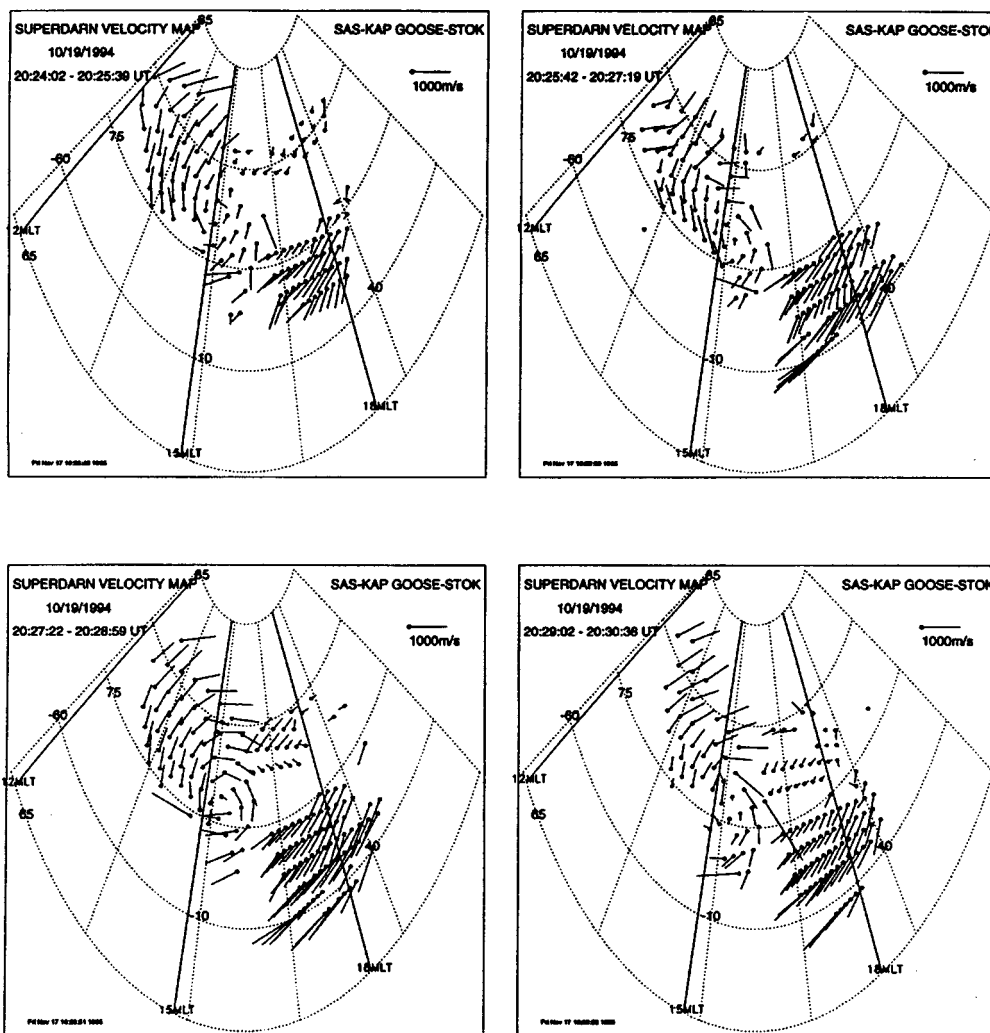


Fig. 4. Four sequential maps of plasma winds over eastern Canada and Greenland as observed at 100 s intervals on 19 October 1994 with the SuperDARN radar network. The maps were obtained in the afternoon local time sector extending from 1200–1900 MLT. Note the dramatic change in the wind patterns on time scales of 100 s, particularly the vortical flow near 15 MLT and 75° magnetic latitude (from Greenwald *et al.* 1996).

3. The SuperDARN Radar Network

The concept of the SuperDARN radar network (Greenwald *et al.* 1995) evolved from discussions amongst scientists in 1991 interested in radar remote sensing of the

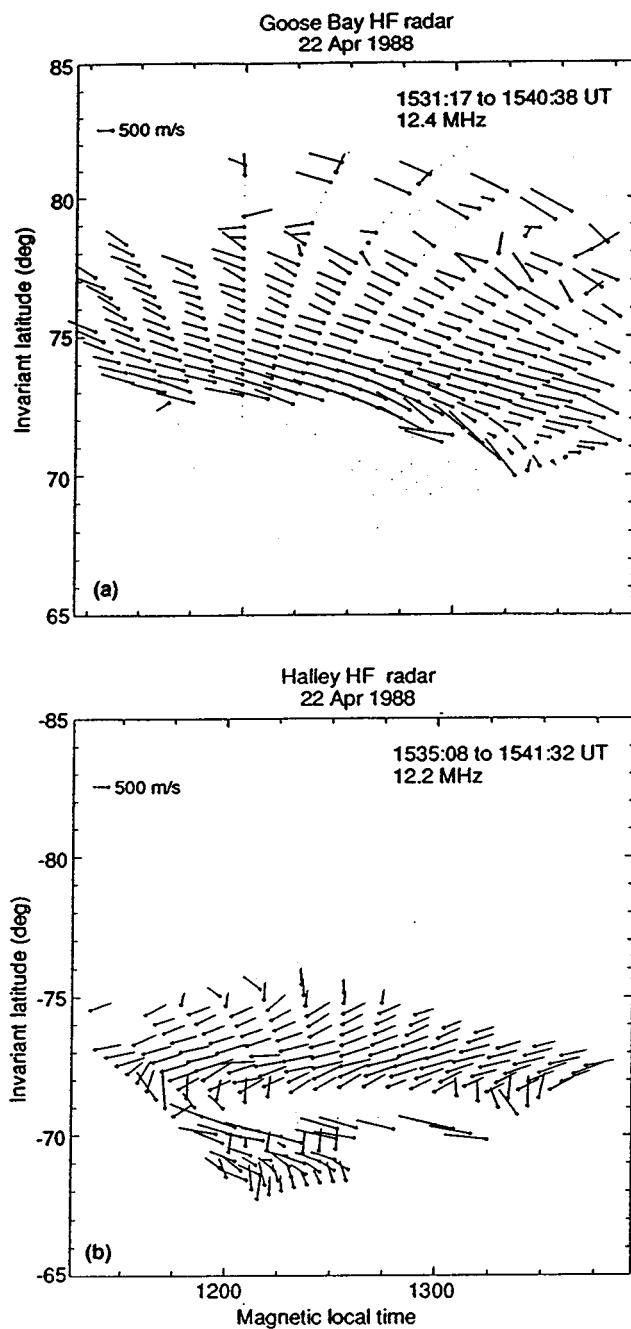


Fig. 5. Simultaneous conjugate observations of F-region plasma drift patterns in the vicinity of the dayside cusp and cleft as observed with the PACE radars at Goose Bay, Labrador and Halley Station, Antarctica. The IMF B_y component was positive and the B_z component was negative at this time (from Greenwald *et al.* 1990).

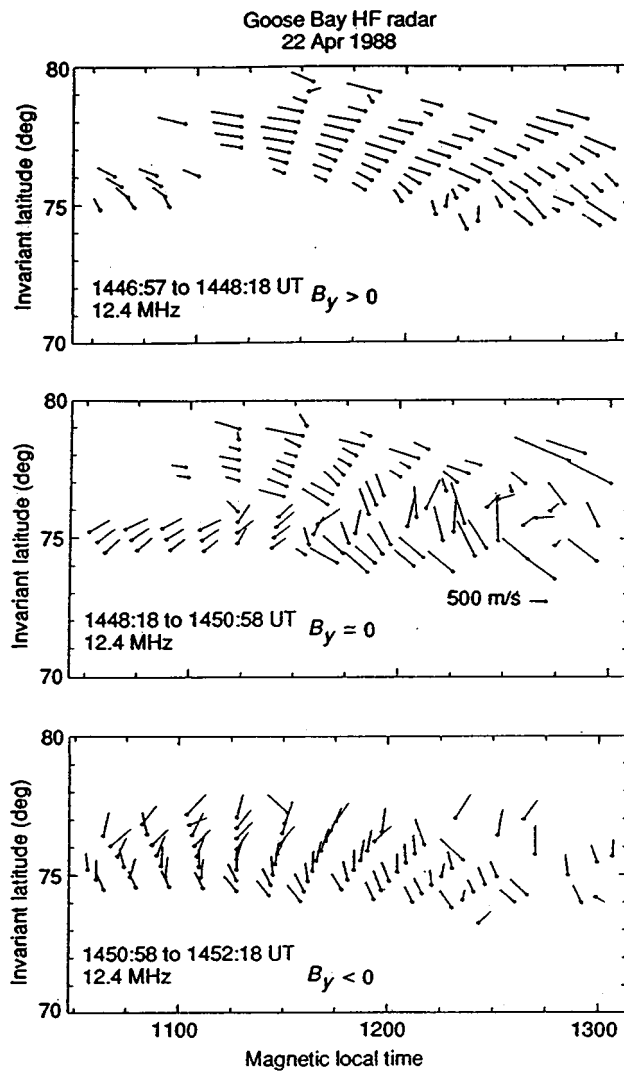


Fig. 6. Goose Bay radar observations of the temporal variation of F-region plasma drift patterns in the vicinity of the cusp and cleft as IMF B_y changes from positive to negative and B_z remains negative (from Greenwald *et al.* 1990).

ionosphere. At the time, it was recognised that a network of paired HF radars could provide extensive spatial coverage and high temporal resolution measurements of plasma winds in the upper atmosphere. A plan was developed to share the responsibility for the development of the new radars and the participants began to prepare proposals to their various funding agencies. While the success was not immediate, it was quite rapid and by late 1992, five new radars were at various levels of construction. The first new pair of radars began operation in 1993 at Saskatoon, Saskatchewan and Kapuskasing, Ontario in Canada, a second radar paired with the existing Goose Bay radar began operation in 1994

at Stokkseyri, Iceland, and a pair of radars began operating from Hankasalmi, Finland and Pykkvibaer, Iceland in 1995. Fig. 7 shows the current constellation of northern-hemisphere SuperDARN radars. Also shown is a recently proposed addition to the northern-hemisphere network that will operate from Soldatna, Alaska. This radar is not yet funded.

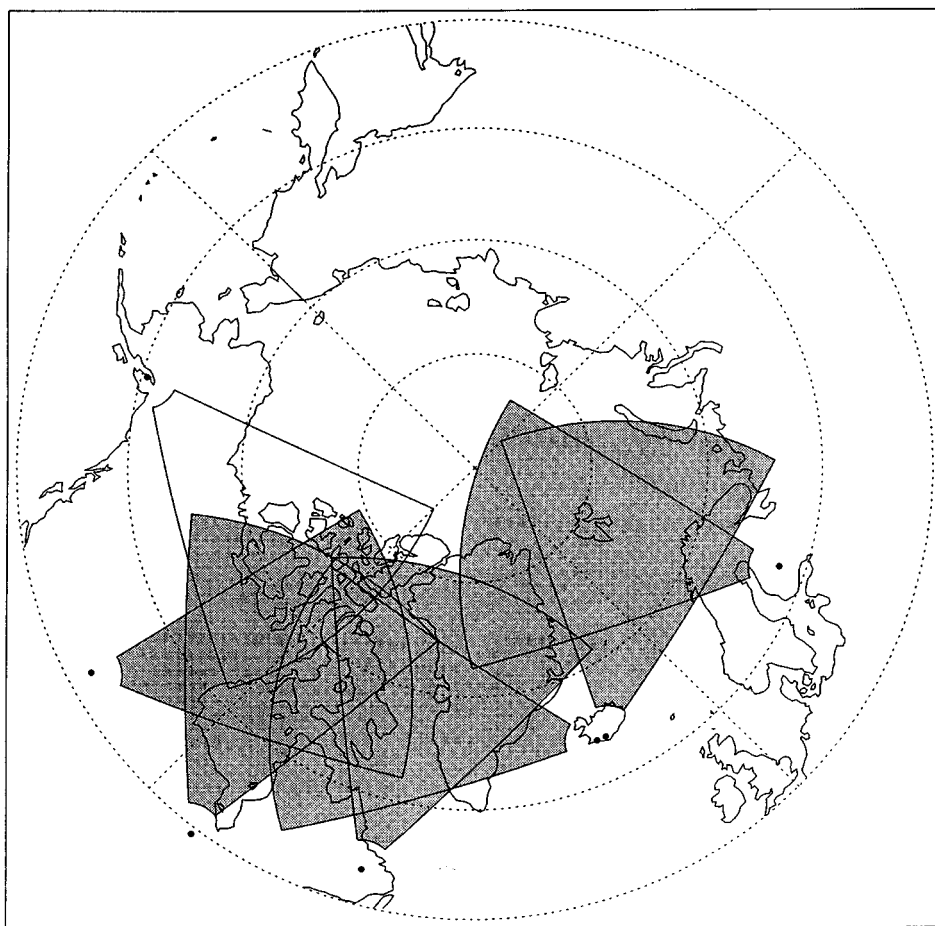


Fig. 7. Fields-of-view of funded (shaded) and planned (unshaded) northern-hemisphere SuperDARN HF radars.

In the southern hemisphere a radar, jointly funded by Britain and the US, has been in operation at Halley Station, Antarctica since 1988. A second radar was constructed by the Japanese at their Syowa base in 1995. It shares a common field-of-view with the Halley radar. A third radar, funded by South Africa, Britain, and the US, is currently being constructed at the South African SANAE base and will begin joint operations with both the Halley and Syowa radars in early 1997. Japanese scientists are also constructing a second radar

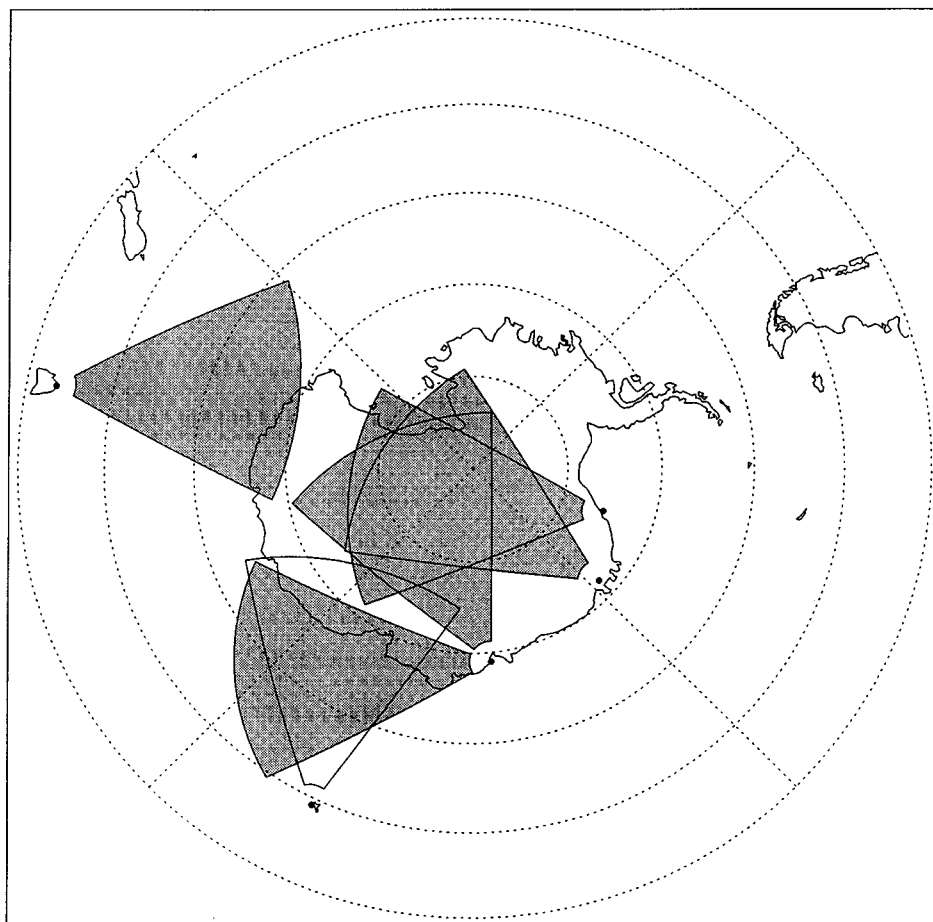


Fig. 8. Fields-of-view of funded (shaded) and planned (unshaded) southern-hemisphere SuperDARN HF radars.

at their Syowa base that will share a common viewing area with a proposed French/Italian/Swedish radar that will be installed at Kerguelan Island. The fields-of-view of all of these radars are shown in Fig. 8. In addition, Fig. 8 shows the field-of-view of the most recently funded element of SuperDARN, the Tasman International Geospace Environment Radar (TIGER). TIGER was funded by the Australian Research Council and is anticipated to begin operation in September 1998. This radar is particularly important for several reasons. First, it will be the only SuperDARN radar operating in this longitude sector in either the northern or southern hemispheres. Second, it is the the only southern-hemisphere radar for which the full data set will be available in near real time. Thirdly, it is located at the lowest magnetic latitude of all SuperDARN radars and will be able to study in more detail the equatorward expansion of the high-latitude convection pattern during strong geomagnetic disturbances. Finally, the TIGER viewing area is separated by twelve hours in local time from the viewing area

of the Halley–SANA E–Syowa radars making it possible to study dawn–dusk and noon–midnight coherencies in the global convection pattern.

SuperDARN is an excellent example of international collaboration in scientific research. At the present time Australia, Britain, Canada, Finland, France, Japan, South Africa, Sweden and the United States are contributing to the international effort. A list of funded radars and the associated Principal Investigators in order of radar deployment date follows:

Northern Hemisphere

Goose Bay, Labrador (53.3° N, –60.5° E)
 Kapuskasing, Ontario (49.4° N, –82.3° E)
 Dr Raymond A. Greenwald
 The Johns Hopkins University Applied Physics
 Lab, USA
 ray_greenwald@jhuapl.edu

Saskatoon, Saskatchewan (52.2° N,
 –106.5° E)
 Prof. George J. Sofko
 Institute of Space and Atmospheric Studies
 University of Saskatchewan, Canada
 sofko@skisas.usask.ca

Stokkseyri, Iceland (63.9° N, –21.0° E)
 Dr Jean-Paul Villain
 Lab Physique et Chimie de L' Environnement
 Terrestre
 Centre Nationale de la Recherche Scientifique,
 France
 jvillain@cnrs-orleans.fr

Hankasalmi, Finland (62.32° N, 26.61° E)
 Pykkvibaer, Iceland (63.86° N, –19.2° E)
 Prof. Tudor B. Jones
 University of Leicester, UK
 tbj@ion.le.ac.uk

Southern Hemisphere

Halley Station, Antarctica (75.5° S,
 –26.6° E)

Dr John R. Dudeney
 British Antarctic Survey, UK
 jrdu@pcmail.nerc-bas.ac.uk

Syowa Station, Antarctica (69.0° S,
 39.6° E)
 Prof. Natsuo Sato
 National Institute of Polar Research, Japan
 nsato@nipr.ac.jp

SANA E Station, Antarctica (71.68° S,
 –2.83° E)

Prof. A. David M. Walker
 Department of Physics
 University of Natal, South Africa
 walker@lola.ph.und.ac.za

Southern Tasmania
 Prof. Peter L. Dyson
 School of Physics
 La Trobe University, Australia
 p.dyson@latrobe.edu.au

A unique feature of the SuperDARN is that all radars are very similar and have been developed to operate from a common base of radar control software. Thus, the data products from the various radars are fully compatible and may readily be viewed with common analysis software. The full data products from the northern-hemisphere radars are regularly sent to The Johns Hopkins University Applied Physics Laboratory where the data are collected onto multiradar exabyte tapes. The tapes are then sent to the University of Saskatchewan where they are copied and distributed to the SuperDARN community for scientific analysis. In this manner, the entire superDARN community has complete access to the total database.

Another feature of SuperDARN is that all of the radars operate continuously. With the exception of the Antarctic sites, the stations are generally unmanned and the radars operate from preplanned monthly schedules. Fifty per cent of the monthly operation is devoted to a common program that scans each radar through 16 adjacent viewing directions on a two-minute schedule. Twenty per cent of the operation is devoted to special operating modes proposed by members of the SuperDARN community. For example, the radars might make high

temporal-resolution observations in a specific viewing direction while scanning through the full azimuth sector more slowly. Finally, 30% of the operation is discretionary to the individual principal investigators and the data obtained during these intervals are initially proprietary. The schedules are generally prepared two months in advance of the month in which they are implemented.

Each of the SuperDARN radars has a design heritage that evolved from the Goose Bay HF radar. All radars have a main antenna array consisting of 16 log-periodic antennas that operate over the frequency range 8–20 MHz. Signals from or to these antennas are phased with electronically-controlled time-delay phasing elements that allow the beam to be steered into 16 directions covering a nominal 52° azimuth sector. The direction of the beams is independent of operating frequency, however the azimuthal resolution of the measurements is dependent on frequency. It ranges from 2.5° at 20 MHz to 6° at 8 MHz. Since most of the observations are made in the frequency range 12–14 MHz, the nominal azimuthal resolution of the radar is $\sim 4^\circ$. At a range of 1500 km, this corresponds to a transverse spatial dimension of ~ 100 km.



Fig. 9. View of antenna arrays of the SuperDARN HF radar located at Kapuskasing, Ontario.

In addition to the main antenna array, a secondary, parallel array of four antennas is used to determine the vertical angle of arrival of the backscattered signal. The second array also uses a phasing matrix and is located 100 m in front of or behind the primary array. It functions as an interferometer to determine the relative phases of the backscattered signals arriving at the two arrays. This phase information is converted to an elevation angle, which is used to determine the propagation modes of the returning signals as a function of range, as well as the approximate altitude of the scatterers. The secondary array is only used for

reception. It does not need to be of the same length as the main array since only the correlated portion of the signals incident on the two arrays is of importance for angle-of-arrival determinations. A view of the SuperDARN antenna arrays at Kapuskasing, Ontario is shown in Fig. 9.

SuperDARN electronic steering occurs on microsecond time scales, allowing the radar to be scanned rapidly through a number of beams or to dwell for an extended period on a single beam. While a wide range of scan sequences are possible, the Goose Bay and Halley radars typically scan in a sequential fashion with a dwell of 7 s in each beam direction. All of the radars are synchronised to begin each scan on two minute boundaries as determined by a Global Positioning System (GPS) clock. The basic northern-hemisphere scan pattern for a pair of radars is for the more westward radar to scan in a clockwise direction and the more eastward radar to scan in a counterclockwise direction. The sense of the scans is reversed for the southern-hemisphere radars. With synchronisation of the viewing direction of the radars, the instantaneous common viewing area will track from north to south during each scan. Other positions within the common field-of-view of the radars will be monitored at different times and therefore be subject to potential error due to short-term temporal variability in ionospheric convection.

Most of the SuperDARN radars use broadband (8–20 MHz) solid state transmitters located in weatherproof containers at the base of each antenna of the main array. Each transmitter has a peak output power ranging from 500–800 W across the frequency band and a duty cycle of up to 6%. The typical pulse length of the transmitted signal is 300 μ s, yielding a range resolution of 45 km. Due to the modest transmitted powers and low duty cycle, less than 2 kW of power is required to operate each radar. This enables the SuperDARN radars to be operated continuously with little regard to the power costs. On the other hand, the peak effective radiated power (ERP) of each radar as computed from the peak pulse power and the antenna gain is in excess of 3 MW.

The radars are controlled by a fast Pentium®-based micro-computer system running a real-time operating system (QNX®, QNX Ltd, Toronto, Canada). This system is extremely flexible and can be used to modify virtually all of the operating parameters of a radar. Changes in operation can be performed directly by an operator, under program control in response to a specific schedule, or under program control in response to changing ionospheric conditions as observed by the radar. A radar can be controlled remotely using a standard telephone modem, enabling very complex experiments to be conducted without an operator actually being located at the radar site. Java-based displays have been developed enabling real-time data to be viewed concurrently by a number of scientists using the world wide web

The SuperDARN radars use a number of different multipulse transmission sequences consisting of 5 to 7 pulses transmitted over a 100 μ s time period. The backscatter returns from these pulses are sampled and processed to produce multi-lag autocorrelation functions (ACFs) as a function of range. A multipulse pattern is a staggered, non-redundant lag sequence from which the backscatter ACFs can be uniquely determined as a function of range. The ACFs are fitted to determine the backscattered power, the mean Doppler velocity, and the width of the Doppler power spectrum for each range where there are significant returns.

These estimates are produced in real-time and stored along with the complete autocorrelations functions on CD-ROM. The fitted data are also available for remote monitoring using the Java-based displays.

4. Summary

In the uppermost reaches of the Earth's atmosphere there are highly dynamic plasma winds which have global-scale dimension and are closely linked with space-weather phenomenology. Large mass ejections from the Sun can interact with the Earth's magnetosphere and ionosphere causing large increases in the magnitude and spatial extent of the plasma winds in the upper atmosphere and potential damage to power distribution systems and communications. In the same way that meteorologists have developed monitoring systems to observe and track weather systems in the lower atmosphere, space scientists are developing monitoring systems to observe and track space-weather disturbances. One of these systems is the SuperDARN radar network which provides the first global-scale observations of the structure and dynamics of plasma winds in the high-latitude ionosphere.

Individuals who are interested in learning more about the SuperDARN network and observations are invited to visit the SuperDARN home page at http://sd-www/RADAR/SD_homepage.html. Much additional information on the SuperDARN network is available as well as extensive on-line data resources. A visitor may also have the opportunity to observe data being acquired from one or more of the radars in real time.

Acknowledgments

This work was supported by NSF Grant ATM-9502993 and NASA Grant NAG5-1099.

References

- Banks, P. M., and Doupnik, J. R. (1975). A review of auroral zone electrodynamics deduced from incoherent scatter radar observations, *J. Atmos. Terr. Phys.* **37**, 951.
- Crooker, N. U. (1992). Reverse convection, *J. Geophys. Res.* **97**, 19363–72.
- Evans, J. V., Holt, J. M., and Wan, R. H. (1979). Millstone Hill incoherent scatter radar observations of auroral convection over $60^\circ \leq \Lambda \leq 75^\circ$, *J. Geophys. Res.* **84**, 7059–74.
- Fahleson, U. (1967). Theory of electric field measurements conducted in the magnetosphere with electric field probes, *Space Sci. Rev.* **7**, 238–62.
- Frank, L. A., and Craven, J. D. (1988). Imaging results from Dynamics Explorer 1, *Rev. Geophys.* **26**, 249.
- Freeman, M. P., Ruohoniemi, J. M., and Greenwald, R. A. (1991). The determination of time-stationary two-dimensional convection patterns with single-station radars, *J. Geophys. Res.* **96**, 15735–49.
- Greenwald, R. A., Baker, K. B., Ruohoniemi, J. M., Dudeney, J. R., Pinnock, M., Mattin, N., Leonard, J. M., and Lepping, R. P. (1990). Simultaneous conjugate observations of dynamic variations in high-latitude dayside convection due to changes in IMF B_y , *J. Geophys. Res.* **95**, 8057–72.
- Greenwald, R. A., Baker, K. B., Dudeney, J. R., Pinnock, M., *et al.* (1995). DARN/SuperDARN: A global view of the dynamics of high-latitude convection, *Space Sci. Rev.* **71**, 761–96.
- Greenwald, R. A., Ruohoniemi, J. M., Bristow, W. A., Sofko, G. J., Villain, J.-P., Huuskonen, A., Kokubun, S., and Frank, L. A. (1996). Mesoscale dayside convection vortices and their relation to substorm phase, *J. Geophys. Res.* **101**, 21697–713.

- Heelis, R. A., Hanson, W. B., Lippincott, C. R., Zuccaro, D. R., Harmon, L. H., Holt, B. J., Doherty, J. E., and Power, R. A. (1981). The drift meter for Dynamics Explorer-B, *Space Sci. Instrum.* **5**, 511–21.
- Heppner, J. P., and Maynard, N. C. (1987). Empirical high-latitude electric field models, *J. Geophys. Res.* **92**, 4467–90.
- Mozer, F. S. (1973). Analyses of techniques for measuring DC and AC electric fields in the magnetosphere, *Space Sci. Rev.* **14**, 272–313.
- Mozer, F. S., and Serlin, R. (1969). Magnetospheric electric field measurements with balloons, *J. Geophys. Res.* **74**, 4739.
- Murphree, J. S., Elphinstone, R. D., Cogger, L. L., and Hearn, D. (1991). In ‘Magnetospheric Substorms’ (Eds J. R. Kan *et al.*), pp. 257–75 (American Geophysical Union: Washington).
- Potemra, T. A. (1994). In ‘Physical Signatures of Magnetospheric Boundary Layer Processes’ (Eds J. A. Holtet and A. Egeland), pp. 3–27 (Kluwer Academic: Netherlands).
- Rich, F. J., and Hairston, M. (1994). Large-scale convection patterns observed by DMSP, *J. Geophys. Res.* **99**, 3827–44.
- Ruohoniemi, J. M., Greenwald, R. A., Baker, K., Villain, J.-P., Hanuise, C., and McCready, M. A. (1987). Drift motions of small-scale irregularities in the high-latitude F-region: An experimental comparison with plasma drift motions, *J. Geophys. Res.* **92**, 4553–64.
- Ruohoniemi, J. M., and Greenwald, R. A. (1996). Statistical patterns of high-latitude convection obtained from Goose Bay radar observations, *J. Geophys. Res.* **101**, 21743–64.
- Wallace, J. M., and Hobbs, P. V. (1977). ‘Atmospheric Science, An Introductory Survey’ (Academic: New York).
- Weimer, D. R. (1995). Models of high-latitude electric potentials derived with a least error fit of spherical harmonic coefficients, *J. Geophys. Res.* **100**, 19595–607.